9400 *Inorg. Chem.* **2010**, *49*, 9400–9408
DOI: 10.1021/ic101103g

Inorganic Chemistry
Article

"Hexagonal Molybdenum Trioxide"—Known for 100 Years and Still a Fount of New Discoveries

Hans-Joachim Lunk,*,† Hans Hartl,‡ Monika A. Hartl,§ Martin J. G. Fait,∥ Ilya G. Shenderovich,‡ Michael Feist,⊥ Timothy A. Frisk,† Luke L. Daemen,§ Daniel Mauder,‡ Reinhard Eckelt,∥ and Andrey A. Gurinov‡

†*Global Tungsten and Powders Corp., Towanda, Pennsylvania 18848,* ‡*Freie Universität Berlin, Germany, D-14195 Berlin, Germany,* §*National Laboratory, Los Alamos, New Mexico 87545,* ∥*Leibniz Institute for Catalysis at Rostock University, D-18059 Rostock, Germany, and* ⊥*Humboldt-Universität zu Berlin, Institut für Chemie, D-12489 Berlin, Germany*

Received June 1, 2010

In 1906, the preparation of "molybdic acid hydrate" was published by Arthur Rosenheim. Over the past 40 years, a multitude of isostructural compounds, which exist within a wide phase range of the system $MoO_3-NH_3-H_2O$, have been published. The reported molecular formulas of "hexagonal molybdenum oxide" varied from MoO_3 to $MoO_3 \cdot 0.33NH_3$ to $MoO_3 \cdot nH_2O$ ($0.09 \leq n \leq 0.69$) to $MoO_3 \cdot mNH_3 \cdot nH_2O$ ($0.09 \leq m \leq 0.20$; $0.18 \leq n \leq 0.60$). Samples, prepared by the acidification route were investigated using thermal analysis coupled online to a mass spectrometer for evolved gas analysis, X-ray powder diffraction, Fourier transform infrared, Raman, magic-angle-spinning ^{1}H- and ^{15}N NMR spectroscopy, and incoherent inelastic neutron scattering. A comprehensive characterization of these samples will lead to a better understanding of their structure and physical properties as well as uncover the underlying relationship between the various compositions. The synthesized polymeric parent samples can be represented by the structural formula $(NH_4)_x{}^3_\infty[Mo_y\square_{1-y}O_{3y}(OH)_x(H_2O)_{m-n}] \cdot nH_2O$ with $0.10 \leq x \leq 0.14$, $0.84 \leq y \leq 0.88$, and $m + n \geq 3 - x - 3y$. The X-ray study of a selected monocrystal confirmed the presence of the well-known 3D framework of edge- and corner-sharing MoO_6 octahedra. The colorless monocrystal crystallizes in the hexagonal system with space group $P6_3/m$, $Z = 6$, and unit cell parameters of $a = 10.527(1)$ Å, $c = 3.7245(7)$ Å, $V = 357.44(8)$ Å^3, and $\rho = 3.73$ g·cm^{-3}. The structure of the prepared monocrystal can best be described by the structural formula $(NH_4)_{0.13}{}^3_\infty[Mo_{0.86}\square_{0.14}O_{2.58}(OH)_{0.13}(H_2O)_{0.29-n}] \cdot nH_2O$, which is consistent with the existence of one vacancy (□) for six molybdenum sites. The sample $MoO_3 \cdot 0.326NH_3 \cdot 0.343H_2O$, prepared by the ammoniation of a partially dehydrated $MoO_3 \cdot 0.170NH_3 \cdot 0.153H_2O$ with dry gaseous ammonia, accommodates NH_3 in the hexagonal tunnels, in addition to $[NH_4]^+$ cations and H_2O. The "chimie douce" reaction of $MoO_3 \cdot 0.155NH_3 \cdot 0.440H_2O$ with a 1:1 mixture of NO/NO_2 at 100 °C resulted in the synthesis of $MoO_3 \cdot 0.539H_2O$. This material is of great interest as a host of various molecules and cations.

Introduction

Transition metal oxides such as molybdenum trioxide, MoO_3, and tungsten trioxide, WO_3, have drawn much attention due to their variety of crystalline phases and their inherent chromogenic properties. These oxides are useful in the fabrication and development of electrochromics, electronic information displays, batteries, optical memory devices, and in sensor device technology.[1,2] Recently, research efforts have been focused on the synthesis and characterization of one- and two-dimensional structures such as ultrathin films, nanorods, nanobelts, and nanofibers,[3] which exhibit properties quite different from the bulk properties of the materials.

It is well-known that the particular phases of nanostructured MoO_3 are highly dependent on the synthetic route. Molybdenum trioxide exhibits five polymorphs. In addition to the thermodynamically stable orthorhombic α-MoO_3 with a peculiar 2D layered structure,[4] four metastable polymorphs have been discovered. The β-MoO_3 and β′-MoO_3 modifications are monoclinically distorted variants of the 3D ReO_3 structure.[5] The high-pressure modification MoO_3-II produces a specific monoclinic ($P2_1/m$) phase.[6] Like the α-MoO_3 structure, the structure of MoO_3-II is layered. In fact, the individual

*To whom correspondence should be addressed. E-mail: hans-joachim.lunk@globaltungsten.com.

(1) Rao, C. N. R.; Raveau, B. *Transition Metal Oxides: Structure, Properties, and Synthesis of Ceramic Oxides*; 2nd ed.; Wiley-Interscience: New York, 2004.
(2) Hosono, K.; Matsubara, L.; Murayama, N.; Woosuck, S.; Izu, N. *Chem. Mater.* **2005**, *17*, 349–354.
(3) Fu, G.; Xu, X.; Lu, X.; Wan, H. *J. Am. Chem. Soc.* **2005**, *127*, 3989–3996.
(4) Kihlborg, L. *Ark. Kemi* **1964**, *21*, 357–364.
(5) McCarron, E. M., III *J. Chem. Soc., Chem. Commun.* **1986**, 336–338.
(6) McCarron, E. M., III; Calabrese, J. C. *J. Solid State Chem.* **1991**, *91*, 121–125.

 Published on Web 09/14/2010

$MoO_{3/3}O_{2/2}O_{1/1}$ layers of MoO_3-II and α-MoO_3 are virtually identical. However, the stacking sequence of the layers of MoO_3-II (aaa) differs from that of α-MoO_3 (aba). This is equated with an improved packing efficiency for the layers of MoO_3-II versus those of α-MoO_3. The hexagonal phase h-MoO_3 ($P6_3/m$ or $P6_3$), distinct among the metastable polymorphs, allows a versatile intercalation chemistry with interesting chemical, electrochemical, electronic, and catalytic properties.[7] Nanosized molybdenum powders can be produced by using this phase as a precursor.[8,9]

The long and puzzling history of "hexagonal molybdenum trioxide" started in 1906, when Arthur Rosenheim described the preparation of a "molybdic acid hydrate".[10] The substance was precipitated by acidification of an aqueous solution of ammonium paramolybdate (APM), $(NH_4)_6[Mo_7O_{24}]\cdot 4H_2O$, with nitric acid. In 1969, Peters et al. utilized Rosenheim's procedure and analyzed the isolated precipitates by chemical and thermal analyses and also by XRD.[11] Depending on the concentration of the starting chemicals APM and HNO_3, the composition of their "ammonium-C-phase", $MoO_3\cdot mNH_3\cdot nH_2O$, varied from $m = 0.15$ to 0.17 and from $n = 0.405$ to 0.505; the X-ray diffractograms were identical. The authors indexed all measured reflections and described the crystal lattice as cubic body-centered {$a = (12.98 \pm 0.02)$ Å}.

Since 1969, a large number of papers have been published about "hexagonal molybdenum trioxide" (HEMO). However, most of the authors overlooked the already existing literature and claimed the syntheses of new phases. The reported overall composition of HEMO varied from MoO_3 to $MoO_3\cdot 0.33NH_3$ to $MoO_3\cdot nH_2O$ ($0.09 \le n \le 0.69$) to $MoO_3\cdot mNH_3\cdot nH_2O$ ($0.09 \le m \le 0.20$; $0.18 \le n \le 0.60$). These phases, characterized by virtually identical XRD's, can be obtained by thermal decomposition of APM;[12,13] by acidification of aqueous solutions of APM or ammonium dimolybdate (ADM), $(NH_4)_2[Mo_2O_7]$;[14] by reaction in a sealed tube between MoO_3, NH_3, and H_2O;[15] and also from MoO_3 and a mixture of ammonium carbamate and ammonium bicarbonate.[16] Kiss et al. first correctly identified the HEMO phase as hexagonal.[12]

Hexagonal molybdenum trioxide thin films with good crystallinity and high purity have been fabricated by a liquid phase deposition technique using molybdenum trioxide monohydrate, $MoO_3\cdot H_2O$, dissolved in hydrofluoric and boric acids as precursors. The synthesized substance belongs to the hexagonal molybdenum oxide hydrate system $MoO_3\cdot nH_2O$ ($n \sim 0.56$). The unit cell parameters were determined to be $a = 10.651$ Å, $c = 3.725$ Å, and $V = 365.997$ Å^3.[17]

Hexagonal molybdenum trioxide hydrate, $Mo_3O_9\cdot H_2O$, has also been synthesized under hydrothermal conditions. The synthesized substance belongs to the hydrate system $MoO_3\cdot nH_2O$ ($n \sim 0.33$). The unit cell parameters are $a = 10.6303$ Å, $c = 3.7215$ Å, and $V = 364.20$ Å^3.[18]

The publication by Ramana et al.[19] does not include the overall composition of the synthesized phase using chemical analysis. Instead, these authors report on the crystal structure and morphology of hexagonal phase MoO_3 nanorods prepared by a simple chemical precipitation route using APM.

Zheng et al.[20] claimed the synthesis of novel metastable hexagonal MoO_3 nanobelts. Even though a mass loss at 300 °C of 5.2% was observed, the existence of pure MoO_3 was still asserted. Sodium nitrate was a component of their preparation method. The authors declared the synthesized product sodium-free. However, they did not verify the absence of Na^+ by analysis. The XRD identification of the "MoO_3" was based on the old, incorrect JCPDS card No. 21-0569 with lattice parameters of $a = 10.53$ Å and $c = 14.97$ Å ($Z = 51$!).

By using the acidification route, even the synthesis of a new cubic heteropolymolybdate with a Keggin-type structure "$(NH_4)_2[MoO_4Mo_{12}O_{36}]\cdot 6H_2O$" was claimed, wherein molybdenum allegedly resides in both the tetrahedral central as well as the octahedral peripheral atomic positions.[8,9] The published X-ray pattern of the rod-shaped crystals is identical with that of HEMO; its overall composition $MoO_3\cdot 0.154NH_3\cdot 0.538H_2O$ lies within the known range of compositions for $MoO_3\cdot mNH_3\cdot nH_2O$.

The hexagonal phase has been verified also for HEMO compositions, containing Na, K, Rb, Cs, or Ag cations[21,22] instead of $[NH_4]^+$ and also for compounds like $H_{0.13}V_{0.13}MoO_{0.87}O_3\cdot 3H_2O$, where a fraction of molybdenum is occupied by vanadium.[23]

All of the molybdenum atoms in the structure of HEMO, discussed above, are in the +6 oxidation state. By using hydroxylamine hydrochloride as a reducing agent, the hexagonal ammonium molybdenum bronze $NH_4Mo_6O_{18}$ [$(NH_4)_{0.17}MoO_3$] was synthesized, producing molybdenum atoms with an average oxidation state of +5.83.[24]

The objective of this work is to dispel the confusion which has arisen in the literature concerning the identity of HEMO phases variously described. A comprehensive characterization of these materials will lead to a better understanding of the structure and physical properties of $MoO_3\cdot mNH_3\cdot nH_2O$, whose composition can vary over a relatively wide range. Preliminary results of our study were presented at the 17th Plansee Seminar.[25]

The targeted synthesis of the HEMO phase has the potential for being utilized as material for intercalation chemistry

(7) Guo, J.; Zavalij, P.; Whittingham, M. S. *Eur. J. Solid State Inorg. Chem.* **1994**, *31*, 833–842.
(8) Singh, R. P.; Wolfe, T. A.; Houck, D. L. Ammonium Dodecamolybdomolybdate and Method of Making, U.S. Patent No. 6,793,907 B1, Sep. 21, 2004.
(9) Singh Gaur, R. P.; Wolfe, T. A. *Proceedings 2006 Int. Conf. Tungsten, Refract. & Hardmetals VI*, Orlando, FL, Feb 7−8, 2006; Metal Powder Industries Federation: Princeton, NJ, 2006; pp 122−131.
(10) Rosenheim, A. *Z. Anorg. Chem.* **1906**, *50*, 320.
(11) Peters, H.; Till, L.; Radeke, K. H. *Z. Anorg. Allg. Chem.* **1969**, *365*, 14–21.
(12) Kiss, A. B.; Gadó, P.; Asztalos, I.; Hegedüs, A. J. *Acta Chem. Acad. Sci. Hung.* **1970**, *66*, 235–249.
(13) Weinhold, J.; Jentoft, R. D.; Ressler, T. *Eur. J. Inorg. Chem.* **2003**, 1058–1071.
(14) Sotani, N. *Bull. Chem. Soc. Jpn.* **1975**, *48*, 1820–1825.
(15) Garin, J. L.; Blanc, J. M. *J. Solid State Chem.* **1985**, *58*, 98–102.
(16) Benchrifa, R. *Ann. Chim. Sci. Mater.* **2007**, *32*, 277–282.
(17) Deki, S.; Béléké, A. B.; Kotani, Y.; Mizuhata, M. *J. Solid State Chem.* **2009**, *182*, 2362–2367.
(18) Zhao, J.; Ma, P.; Wang, J.; Niu, J. *Chem. Lett.* **2009**, *38*, 694–695.
(19) Ramana, C. V.; Atuchin, V. V.; Troitskaia, I. B.; Gromilov, S. A.; Kostrovsky, V. G.; Saupe, G. B. *Solid State Commun.* **2009**, *149*, 6–9.
(20) Zheng, L.; Xu, Y.; Jin, D.; Xie, Y. *Chem. Mater.* **2009**, *21*, 5681–5690.
(21) Guo, J.; Zavalij, P.; Whittingham, M. S. *J. Solid State Chem.* **1995**, *117*, 323–332.
(22) McCarron, E., III; Thomas, D. M.; Calabrese, J. C. *Inorg. Chem.* **1987**, *26*, 370–373.
(23) Dupont, L.; Larcher, D.; Portemer, F.; Figlarz, M. *J. Solid State Chem.* **1996**, *121*, 339–349.
(24) Jiang, C.-C.; Liu, G.; Wei, Y.-G.; Wang, W.; Zhang, S.-W. *Inorg. Chem. Commun.* **1999**, *2*, 258–260.
(25) Lunk, H.-J.; Hartl, H.; Frisk, T. A.; Shenderovich, I. G.; Mauder, D.; Feist, M.; Fait, M. F. G.; Hartl, M. A.; Daemen, L. L.; Eckelt, R. *Proceedings 17th International Plansee Seminar*, Reutte, Tirol, Austria, May 25−29, 2009, GT 2/1−14; Sigl, L. S., Ed.; Plansee Group: Reutte, Tirol, Austria, 2009; Vol. *3*.

Table 1. Overall Composition and X-Ray Characterization of h-MoO_3 Samples

					$MoO_3 \cdot oNH_3 \cdot pH_2O$			(Å)	
parent sample	preparation	processed sample	preparation	NH_3 (%)	o	p	$o+p$	a	c
h-MoO_3-1	ADM + aqua regia			1.58	0.143	0.440	0.583	10.58	3.73
h-MoO_3-1		h-MoO_3-1−300	heating at 300 °C	1.59	0.141	0.253	0.394	10.58	3.72
		h-MoO_3-1-320	heating at 320 °C	1.32	0.116	0.211	0.327	10.59	3.73
		h-MoO_3-1-P	drying over P_4O_{10}	1.70	0.153	0.372	0.525	10.58	3.73
h-MoO_3-1-P		h-MoO_3-1-NH_3	ammoniation with dry NH_3	3.57	0.326	0.343	0.669	10.54	3.73
h-MoO_3-2	ADM + aqua regia			1.71	0.155	0.440	0.595	10.56	3.73
h-MoO_3-2		h-MoO_3-2-NOX	"chimie douce" reaction with NO/NO_2	< 0.2	0.000	0.539	0.539	10.59	3.72
h-MoO_3-3	ADM + HCl			1.82	0.161	0.243	0.404	10.59	3.72
h-MoO_3-15N	ADM + $^{15}NH_4NO_3$ + HNO_3			1.20	0.108	0.425	0.533	10.55	3.72

and different catalytic applications. Its reduced form can be used as a starting material for making nanosized molybdenum metal and molybdenum carbide powders.[8,9]

Experimental Section

Preparation. The preparation followed the route taken by the authors of ref 9. The starting chemical, ADM, was manufactured at Global Tungsten & Powders Corp. (GTP) in Towanda, Pennsylvania. Its trace element concentrations in parts per million were as follows: Ca, Mg < 1; Mn, Ni < 2; Al, Cr, Cu, Fe < 4; Na < 5; Pb < 6; As, Si, Sn, P < 8; W = 65; K = 95. The apparent Scott density amounted to 1.34 g/cm^3. A quantity of 38 g of ADM was dissolved in 400 mL of deionized water and heated to about 70 °C. While agitating the solution with a magnetic stirrer, 150 mL of aqua regia (three parts 12N HCl, one part 14N HNO_3, by volume) was added. Then, 100 mL of a diluted aqueous ammonia solution (one part 14N NH_3 to one part water) was added, while continuously stirring. The clear solution had a light yellow color, and the desired phase was precipitated by adding 40 mL of 14N HNO_3, while continuously stirring. After about 15 min, a colorless precipitate formed. The precipitate was left in the mother liquor overnight and then isolated by filtration. The precipitates h-MoO_3-1 and h-MoO_3-2 (see Table 1) were washed once with 200 mL of 0.1N HNO_3 and three times with deionized water and then dried at 110 °C. Alternatively, the precipitate was fabricated using only 3.3N HCl, instead of aqua regia (h-MoO_3-3).

To prepare monocrystals, the solution was heated at 70 °C for another 5 to 10 min and then left to crystallize. So, the stirring and vibrations at the last step of the synthesis are avoided, the nucleation decelerates, and the isolation of small single crystals is achieved.

For synthesizing a small ^{15}N-containing sample, the preparation was modified as follows. Quantities of 2.54 g of ADM, 0.91 g of $^{15}NH_4NO_3$, and 1.47 g of $^{14}NH_4NO_3$ were dissolved in 35 mL of deionized water and heated to about 70 °C. While agitating the solution with a magnetic stirrer, 10 mL of 14N HNO_3 were added. Then, 6.6 mL of a diluted aqueous ammonia solution was added, while continuously stirring. The desired phase h-MoO_3-15N was precipitated by adding 2.66 mL of 14N HNO_3, while continuously stirring. The subsequent steps followed the route described above.

The sample h-MoO_3-1-NH_3 was prepared by the ammoniation of a partially dehydrated h-MoO_3-1 with dry gaseous ammonia.

The "chimie douce" reaction of HEMO with NO/NO_2 was performed in an integral fixed bed reactor made from fused silica (i.d. 10 mm; isothermal heating zone 50 mm; PID controller) at 100 °C, and the sample mass was 1.00 g. The educt feed was a 1:1 mixture of NO and NO_2 (diluted in He, each 0.5%, 20 mL·min^{-1}) in He (30 mL·min^{-1}). Before feeding the reactor with the reaction gas mixture, the sample was treated in He at 100 °C for 2−3 h to equilibrate the educt flow and to stabilize the multigas sensor. After the desired reaction time, the educt mixture was replaced by helium. The composition of the educt and product stream was analyzed by an online multigas sensor (Analyzer AO2020, Asea Brown Boveri AG, Mannheim, Germany) for the simultaneous analysis of NO and NO_2.

Instrumentation and Analytical Procedures. The dried precipitates were characterized by chemical analysis, scanning electron microscopy (SEM), X-ray diffraction (XRD), thermal analysis coupled online by a *Skimmer* system to a quadrupole mass spectrometer for evolved gas analysis (TA-MS), Fourier-transform infrared (FTIR), Raman and solid-state magic-angle-spinning (MAS) ^1H- and ^{15}N NMR spectroscopy, and also by incoherent inelastic neutron scattering (IINS).

For determining the molar composition $MoO_3 \cdot oNH_3 \cdot pH_2O$ of the precipitated samples, two independent analytical measurements were needed. The content of NH_3 was determined by the classical Kjeldahl method.[26] The samples were distilled using a KJELTEC System 1026 Distilling Unit, whereby 100 to 500 mg of the samples were placed into a 100 mL distilling flask to which 10 mL of water and 20 mL of 10N NaOH were added. The sample was then distilled through steam generation for 3.7 min. The ammonia distillate was collected in a 20 mL solution of saturated boric acid. The collected solution was then titrated on a Mettler DL-67 autotitrator using 0.4N HCl.

By using a Mettler small furnace (SF1100) TGA/SDTA 851e instrument, the mass loss of ~25 mg of sample heated in the air up to 550 °C provides the sum of H_2O and NH_3. The content of H_2O was calculated as the difference of the overall mass loss less the content of NH_3.

A Hitachi S-3000N scanning electron microscope (SEM) was used to acquire images of the powders at an accelerating voltage of 3 kV and a magnification of 5000×.

For the X-ray powder diffraction measurements, a Rigaku D/Max Vertical Goniometer diffractometer was employed. The experimental conditions were as follows: scan range, 6−70 ° 2-θ; step size, 0.02 ° 2-θ; dwell time, 1 s.

The diffraction intensities for the X-ray crystal structure determination measured on a Bruker XPS diffractometer: CCD area detector; Mo Kα radiation (λ = 0.71073 Å; graphite monochromator); T = 173 K; data collection range 2.23° < θ < 30.45°, 2923 collected reflections, 415 unique reflections, 379 reflections with $I > 2\sigma(I)$, R_{int} = 0.019; empirical absorption correction (SADABS); crystal dimensions (mm) 0.1 × 0.1 × 0.06. The structure was solved by direct methods and refined on the basis of F^2 data with a least-squares procedure using the WinGX program system.[27] Anisotropic displacement parameters were assigned to all atoms with the exception of the disordered atoms; hydrogen atoms could not be reliably located. The resulting R values are R_1 [$I > 2\sigma(I)$] = 0.0203; wR_2 [$I > 2\sigma(I)$] = 0.0512; R_1 (all data) = 0.0239; wR_2 (all data) = 0.0528; largest differences ± (e·Å^{-3}) −0.64/1.15.

The TA-MS analysis was performed using an STA 409C thermal analyzer (Netzsch Gerätebau GmbH, Selb/Germany),

(26) Jander, G.; Jahr, K. F. *Massanalyse, Theorie und Praxis der Klassischen und der Elektrochemischen Titrierverfahren*; Walter DE Gruyter & Co.: Berlin, 1959; p 158.

(27) Farrugia, L. J. *J. Appl. Crystallogr.* **1999**, *32*, 837–838.

which was coupled to a quadrupole mass spectrometer (QMG 422, Balzers). The conditions were as follows: 70 mL·min^{-1} air flow; 5 K·min^{-1} heating rate; about 50 mg sample mass; corundum crucibles. The overlapping individual steps have been distinguished by their minima in the DTG curve. The ion current (IC) curves for the selected ions, whose mass to charge ratios (m/z) were 15 (NH^+), 17 (OH^+; NH_3^+), and 18 (H_2O^+), were recorded in the multiple ion detection (MID) mode.

The FTIR spectra were acquired on a Nicolet Magna 760 spectrometer. The samples were dispersed in KBr at a mass ratio of 1:15 using a KBr beamsplitter and a DTGS detector. They were analyzed using the diffuse reflectance infrared Fourier-transform (DRIFT) component. Each FTIR spectrum is a composite of 512 scans at a resolution of 4 cm^{-1}.

The Raman spectra were acquired using a Nicolet 590 Raman module. The samples were analyzed neat in NMR tubes using a CaF_2 beamsplitter and an InGaAs detector. The spectra were acquired using a laser beam of 1.16 W and a resolution of 4 cm^{-1}. Each spectrum was composed of 128 scans.

Incoherent inelastic neutron scattering (IINS) data were collected at a temperature of 10 K on the filter difference spectrometer (FDS) at the LANSCE facility at Los Alamos National Laboratory. This instrument is used for vibrational spectroscopy through incoherent inelastic neutron scattering. The instrument is designed for high count rates using a large solid-angle (3 steradians) detector. The samples were loaded in cylindrical aluminum cans (20 mm outer diameter, 2 mm wall thickness, 100 mm height) in a helium atmosphere to ensure good thermal contact with the closed-cycle refrigerator. After a short temperature equilibration time, a vibrational spectrum was collected over a period of 12 h.

Solid-State High-Resolution ^{1}H and ^{15}N NMR Spectroscopy. The ^{1}H NMR spectra were measured at room temperature, using a 600 MHz (14.1 T) Varian spectrometer, equipped with a Chemagnetics-Varian 3.2 mm pencil MAS probe. The magic-angle-spinning (MAS) rotational frequency was 20 kHz. The ^{1}H-90° pulse length was 1.3 μs. The pulse delay was 4 s, and the number of scans was 256 for all samples. The ^{1}H chemical shifts were referenced to the external standard adamantane (1.74 ppm from TMS).

The ^{15}N NMR measurements were performed on a Bruker MSL-300 instrument operating at 7 T, equipped with a Chemagnetics-Varian 6 mm pencil CPMAS probe. The $\{^1H\}^{15}N$ CPMAS spectra were recorded at room temperature using a cross-polarization contact time of 5 ms, and the typical 90° pulse lengths were about 3.5 μs. The repetition time of the measurements was 5 s. The sample was spun at 6 kHz under MAS conditions. The ^{15}N chemical shift value is referenced to the $CH_3{}^{15}NO_2$ scale.

Results and Discussion

The preparation of HEMO was carried out by using ADM as starting material and aqua regia or HCl or HNO_3. The data from the chemical analysis and X-ray characterization are summarized in Table 1.

The scanning electron microscopy (SEM) image of sample h-MoO_3-1 is shown in Figure 1. The crystals have the shape of straight hexagonal rods.

The X-ray diffractogram of sample h-MoO_3-1 is shown in Figure 2. It is evident that the material is well-crystallized and single-phased. All of the observed reflections can be indexed in hexagonal symmetry, with interplanar spacings reported for h-MoO_3.[12] All samples presented in Table 1 are characterized by an X-ray diffractogram virtually identical with that presented in Figure 2.

The structure remained unchanged, even after heating the sample h-MoO_3-1 to 320 °C (h-MoO_3-1-320) or loading a sample, which was partially dehydrated over P_4O_{10} (h-MoO_3-1-P) with dry gaseous ammonia (h-MoO_3-1-NH_3). The cell parameter a, determined from the powder XRDs, varies from 10.54 to 10.59 Å; parameter c amounted to 3.72−3.73 Å.

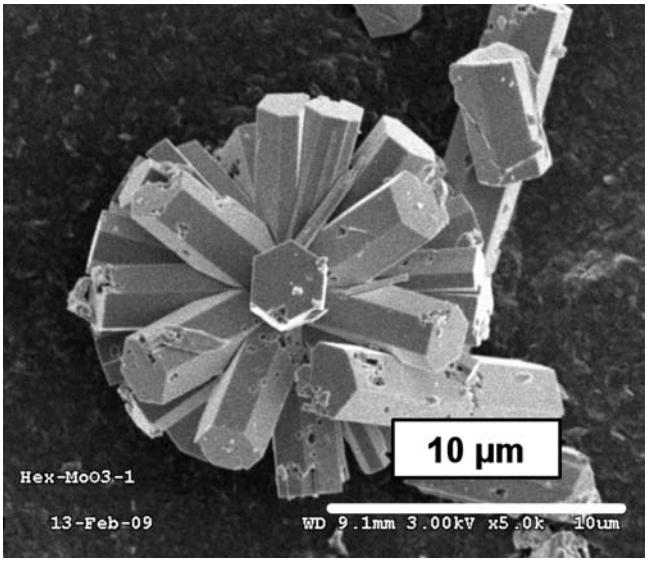

Figure 1. SEM image of h-MoO_3-1.

The X-ray study of a selected colorless monocrystal with the molecular formula $MoO_3 \cdot 0.155NH_3 \cdot 0.490H_2O$ confirmed the presence of the well-known framework of edge- and corner-sharing MoO_6 octahedra with tunnels parallel to [0 0 1], first determined for hexagonal $KMo_5O_{15}OH \cdot 2H_2O$[28] and $(NH_4)Mo_{5.5}O_{17}OH \cdot H_2O$.[16] The compound crystallizes in the hexagonal system with space group $P6_3/m$, $Z = 6$, and unit cell parameters of $a = 10.527(1)$, $c = 3.7245(7)$ Å, $V = 357.44(8)$ Å^3, and $\rho = 3.73$ g·cm^{-3} (Figure 3a and b). The formula of the polymeric compound is estimated on the basis of the crystal structure analysis, and its chemical analysis and can be represented as $(NH_4)_{0.13}{}^3_\infty[Mo_{0.86}\square_{0.14}O_{2.58}(OH)_{0.13}(H_2O)_{0.29-n}] \cdot nH_2O$. It is consistent with the existence of one vacancy (□) for six molybdenum sites. The components NH_4^+ and H_2O outside the square brackets are located in the tunnels. The analytically determined amount of water is situated both in the framework and in the tunnels. We favor this formula over the notation as a pentamolybdate[29] or decamolybdate.[28] The Mo−O bond lengths do not differ significantly from the published values.[16,28] The shortest O···O distance between diagonally located O1 atoms is 5.96 Å. After subtracting the 2-fold van der Waals radius of O or O^{2-}, the diameter of an inserted cylinder becomes 2.5−3.0 Å. The electron density inside of the tunnels is characteristic for disordered nitrogen or oxygen atoms. The O and N atoms are randomly distributed on positions 0 0 0 (site symmetry −6) and 0 0 0.25 (site symmetry −3) with z as the tunnel's axis. The mean N···O and O···O distances of 2.98 Å and 2.83 Å correspond with the lengths of possible hydrogen bonds N−H···O and O−H···O between embedded NH_4^+ or H_2O and the oxygen atoms of the tunnel's wall. The N or O atoms in the tunnel occupy the positions $z = 0$, $z = 0.25$, $z = 0.5$, and $z = 0.75$. Neglecting the calculated nonrealistic short N···N and N···O distances of 0.93 Å and 1.86 Å, there remains a reasonable distance of 2.79 Å. This value is in good agreement with the ionic diameter

(28) Krebs, B.; Paulat-Böschen, I. *Acta Crystallogr.* **1976**, *B32*, 1697–1704.
(29) Slade, R. C. T.; Hall, G. P.; Ramanan, A.; Nicol, J. M. *J. Chem. Soc., Faraday Trans.* **1994**, *90*, 3579–3584.

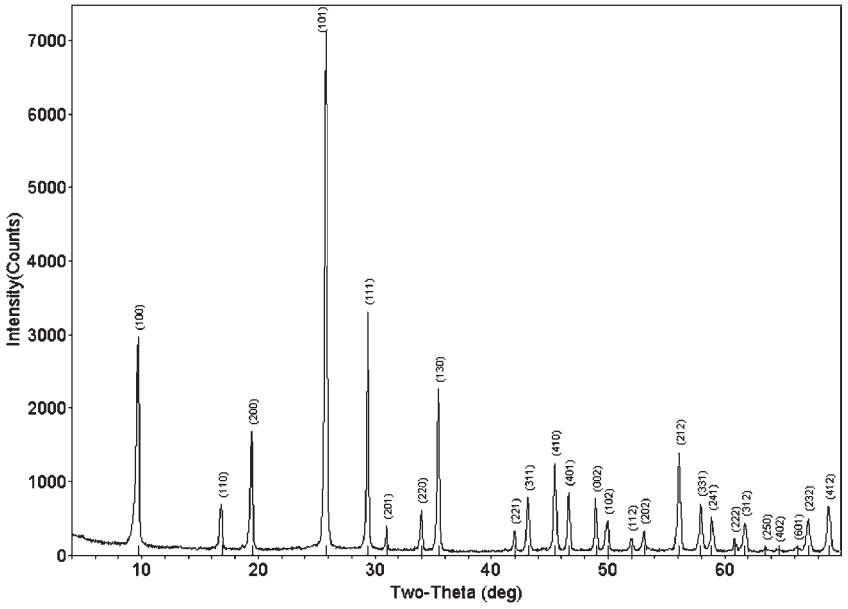

Figure 2. X-ray diffractogram of h-MoO_3-1.

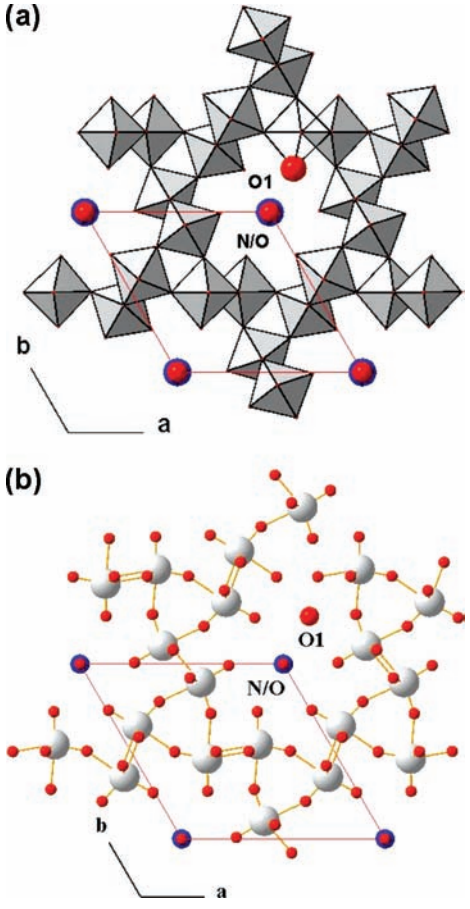

Figure 3. Polyhedral (a) and ball-and-stick (b) representation of the h-MoO_3 framework (view along [0 0 1]) with one missing Mo atom (blank octahedron) and the liberated oxygen atom O1 on a randomly selected position. The channels are occupied by nitrogen/oxygen atoms in the positions 0 0 z (blue, nitrogen; red, oxygen).

of NH_4^+ (2.86 Å). Either value allows only an occupation of 65% of the crystallographically required two ions regarding the translational period of c = 3.724 Å. This occupation value

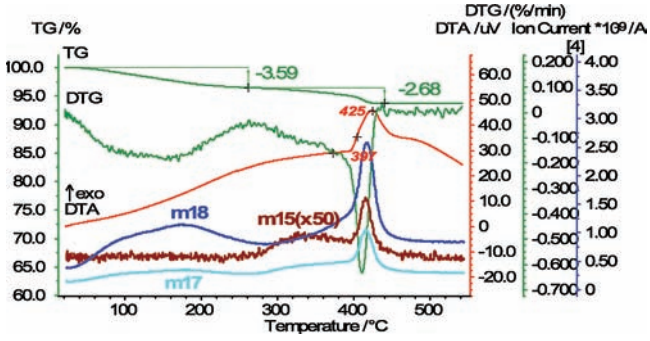

Figure 4. TA-MS curves of h-MoO_3-1 in the air with the ion current (IC) curves for the mass to charge ratios m/z = 15 ($^{15}N^+$), 17 ($^{14}NH_3^+$, OH^+), and 18 (H_2O^+).

resulting from geometrical considerations matches very well with the sum of the population parameters (PP) of O and N of ca. 0.68, determined by the crystal structure analysis.

The PP of Mo was refined to 0.86, whereas the refinement of the PP of the O atoms showed only an insignificant deviation of at most 1.00 ± 0.03. That means that it is impossible to balance the positive charge +0.84 of the missing 0.14 Mo atoms, even if all H_2O molecules were protonated. The surplus negative charge will be compensated by protonation of the terminating O1 atoms, which, due to the missing Mo atoms, would be isolated O^{2-} ions.

The thermal behavior of h-MoO_3-1 in the air is characterized by a sequence of three, possibly four (cf. the two submaxima in the first broad peak, Figure 4), consecutive steps that more or less strongly overlap. All steps are caused by the release of water, while the latter two also show an ammonia liberation with maxima around 340 and 410 °C. Because the contribution of NH_3^+ to the mass to charge (m/z) ratio 17 cannot be significantly differentiated from the OH^+ portion of this ratio, the m/z ratios 17:18 (H_2O^+) cannot be used to determine the amount of liberated ammonia. However, the m/z = 15 (NH^+) trace unambiguously demonstrates the release of ammonia above 280 °C.

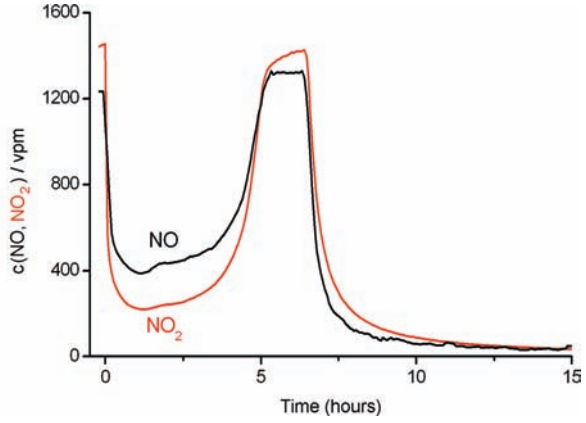

Figure 5. "Chimie douce" reaction of h-MoO_3-2 with a 1:1 mixture of NO/NO_2 at 100 °C.

The thermal characteristics confirmed that the rate of decomposing and removing $[NH_4]^+$ ions is less than that of neutral water molecules at relatively low temperatures. The partial dehydration of h-MoO_3-1 at 300 °C or at room temperature over P_4O_{10} confirmed this finding; at 320 °C, an 18% loss of "ammonia" was observed (cf. Table 1). The general character of the first three mass loss steps is endothermic, as expected (more clearly observed in argon, but not discussed in this contribution), even if the peaks are weak and poorly expressed. This is obviously due to the usage of corundum crucibles, which are preferred when measuring in air (cf. ref 30 where the exothermicity of DTA traces had been attributed to the catalytic oxidation of ammonia in the presence of platinum as crucible material). The third mass loss with the sharp DTG peak at 425 °C is strongly exothermic, which is attributed to the recrystallization of the decomposed parent phase to α-MoO_3. The light gray residue was identified by XRD as orthorhombic α-MoO_3. Regarding the general curve shape of the TG and DTG traces, the behavior in argon is quite similar, except for a somewhat greater mass loss for the temperatures above 250 °C (4.04 vs 2.68%). In argon, the liberated ammonia acts as a reducing agent. The blue-colored residue also contains the molybdenum suboxide Mo_4O_{11}, in addition to the main component α-MoO_3. Both phases were detected by X-ray diffraction.

For the first time, NO_2 was used to prepare hexagonal WO_3 by a "chimie douce" reaction with $(NH_4)_xWO_3$.[31] The "chimie douce" reaction of h-MoO_3-2 with a 1:1 mixture of NO and NO_2 at 100 °C (cf. Preparation section in the Experimental Section) led to the $[NH_4]^+$-free sample h-MoO_3-2-NOX (see Table 1). Figure 5 reveals that both gases react simultaneously with the starting material. The equimolar mixture of the oxidizing agents NO (oxidation state of N +2) and NO_2 (oxidation state of N +4) is the ideal oxidant for the oxidation of $[NH_4]^+$ (oxidation state of N −3) to N_2 with an oxidation state of ±0. The resultant compound is characterized by an X-ray pattern, virtually identical to that of the starting material. The characterization of h-MoO_3-2-NOX by FTIR/Raman spectroscopies and IINS is presented below. From a mechanistic standpoint, the applied "chimie douce" route at 100 °C with an equimolar mixture of NO and NO_2 represents a less complex gas−solid reaction than the use of NO_2 alone at 250 °C.[32] The transformation of h-MoO_3-2 into h-MoO_3-2-NOX requires certain structural rearrangements to eliminate the Mo vacancies in the parent material.

The FTIR spectrum of h-MoO_3-2 is shown in Figure 6; its Raman spectrum is in Figure 7. The bands at 3527 and 1607 cm^{-1} can be attributed to the OH stretching and deformation vibrations of H_2O, respectively. The bands at 3228 and 1435 cm^{-1} agree with the frequencies of the stretching and deformation vibrations of $[NH_4]^+$ ions.[33] In the range below 1000 cm^{-1}, the spectrum shows relatively sharp bands at 971 and 914 cm^{-1} and an absorption at 711 and 523 cm^{-1}, which can be assigned to Mo−O bond stretching and bending vibrations and to the vibrational motion of H_2O. The Raman spectrum also shows the sharp band at 973 cm^{-1} and the broad band at 900 cm^{-1}. Additional bands are observed in the range from 700 to 100 cm^{-1}.

The FTIR spectrum of h-MoO_3-2-NOX clearly indicates that ammonium ions are not present in that sample. The characteristic bands at 3228 and 1435 cm^{-1} are absent (Figure 6). These findings agree with the results of the chemical analysis (cf. Table 1). Compared to the parent material, the Raman spectrum of the $[NH_4]^+$-free sample shows a bathochromic shift of the band at 973 to 981 cm^{-1} (Figure 7).

The IINS spectra were deconvoluted with the instrument resolution function after subtracting a background obtained from a vanadium sample (incoherent scatterer). A comparison of the hexagonal phases h-MoO_3-1, h-MoO_3-320, and h-MoO_3-1-NH_3 (cf. Table 1) to α-MoO_3 is shown in Figures 8−10 at low, medium, and high wave numbers, respectively. A detailed view of two of the more interesting areas is given in Figure 11. Slade et al. published an IINS spectrum of $(NH_4)Mo_{5.33}H_3O_{18}$ in 1994.[29] Their band assignments agree well with ours, but we had the advantage of being able to measure at higher frequencies and observed the O−H and N−H stretching that appears at wave numbers above 3000 cm^{-1}. The bands that appear in all four samples are due to Mo−O vibrations of the molybdenum oxides. The extra bands in the three hexagonal samples are due to vibrations of groups containing hydrogen.

The assignment of bands to water and $[NH_4]^+$ cations at low wave numbers was done by comparing the relative intensity of bands for the three hexagonal samples (see Figure 8). Since these samples vary in the amount of ammonia and water they contain, a partial assignment could be done. Librational modes of $[NH_4]^+$ (rotational motion of the cation on its site) give rise to bands at 320 and 359 cm^{-1} comparable to those found in ammonium bromide, $[NH_4]Br$.[33,34] The main librational mode of NH_3 normally appears at a lower frequency, ∼280 cm^{-1}. Notice that librational modes are seldom Raman- or IR-active. Several MoO_3 lattice modes appear at low frequencies. Notice that IINS samples the entire Brillouin zone as opposed to only the Γ point as in Raman or IR spectroscopy. In Figure 8, an increase in intensity is visible between 250 and 450 cm^{-1} from the bottom curve to the top one. This increase in intensity correlates with an increased amount of water in the sample

(30) Fait, M. J. G.; Lunk, H.-J.; Feist, M.; Schneider, M.; Dann, J. N.; Frisk, T. A. *Thermochim. Acta* **2008**, *469*, 12–22.
(31) Petit, S.; Doumerc, J.-P.; Grenier, J.-C.; Seguelong, T.; Pouchard, M. *C. R. Acad. Sci. Paris* **1995**, *321*, Série IIb, 37−41.
(32) Muraoka, Y.; Grenier, J.-C.; Petit, S.; Pouchard, M. *Solid State Sci.* **1999**, *1*, 133–148.
(33) Nakamoto, K. *Infrared and Raman Spectra of Inorganic and Coordination Compounds*; 3rd ed.; John-Wiley and Sons, Inc.: New York, 1978.
(34) Mitchell, P. C. H.; Parker, S. F.; Ramirez-Cuesta, A. J.; Tomkinson, J. *Serie on Neutron Techniques and Applications − Vol. 3: Vibrational Spectroscopy with Neutrons*; World Scientific Publ. Co. Pte. Ltd.: River Edge, NJ, 2005; pp 185−195.

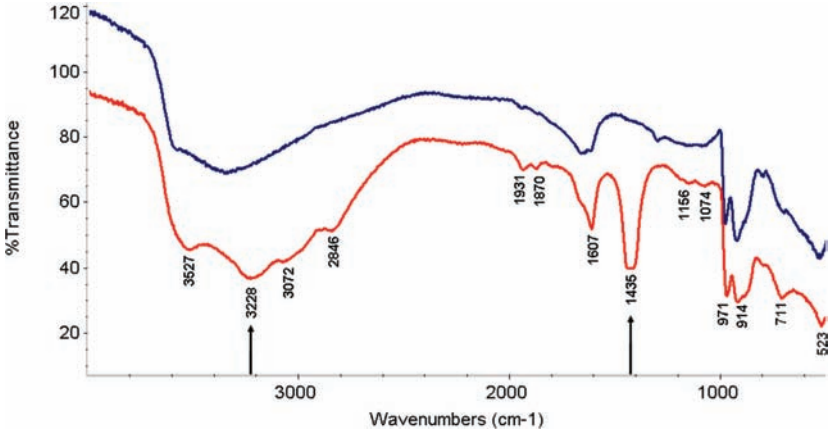

Figure 6. FTIR spectra of h-MoO_3-2 (red) and h-MoO_3-2-NOX (blue).

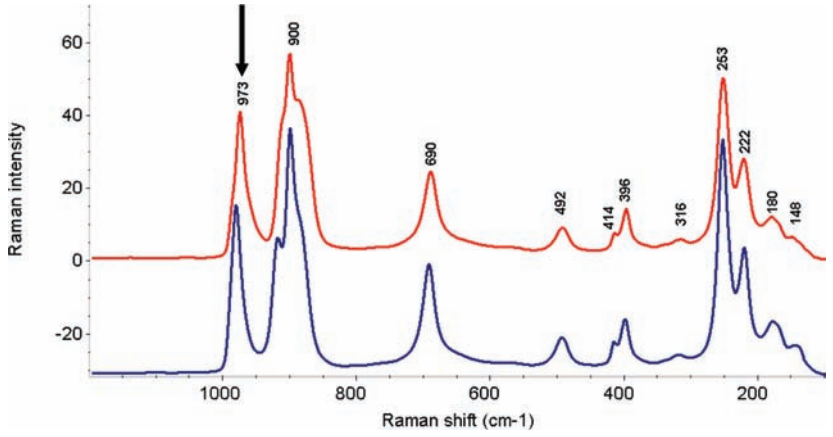

Figure 7. Raman spectra of h-MoO_3-2 (red) and h-MoO_3-2-NOX (blue).

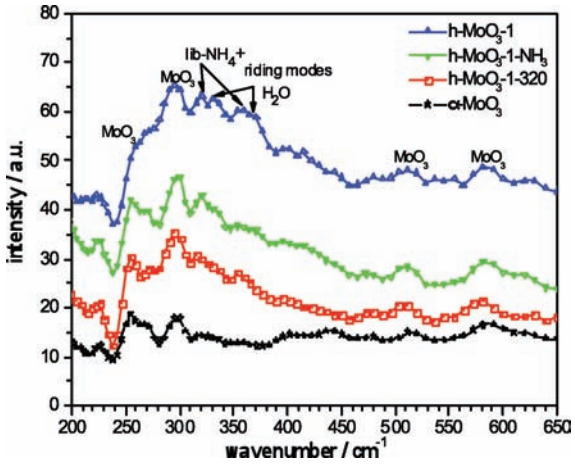

Figure 8. IINS spectra of hexagonal and orthorhombic MoO_3 (low wave number region).

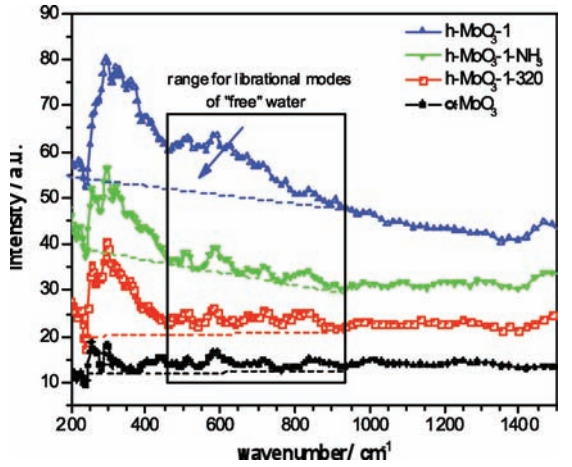

Figure 9. IINS spectra of hexagonal and orthorhombic MoO_3 (medium wave number region).

from the bottom curve (no water) to the top curve ($p = 0.440$). A slight increase in the intensity of MoO_3 lattice modes is also visible. This is likely due to adsorbed water (hydrogen-rich) molecules "riding" the MoO_3 lattice modes. Indeed, to first order, the neutron vibrational spectrum is dominated by the motion of hydrogen atoms thanks to the large incoherent scattering cross-section of hydrogen (80 barns). Molybdenum is a reasonably strong scatterer and will also contribute scattering intensity to the spectrum.

Figure 9 shows the spectra in the medium wave number region. The librational bands for "free" water, i.e., water that is neither complexed nor bound or adsorbed, are usually visible between 550 (librational edge) and 1000 cm^{-1} (box in Figure 9).[35] To clarify the graph, a straight line is drawn underneath each spectrum as a background in the respective color. Only in the

(35) Ockwig, N. W.; Cygan, R. T.; Hartl, M. A.; Daemen, L. L.; Nenoff, T. M. *J. Phys. Chem. C* **2008**, *112*, 13629−13634.

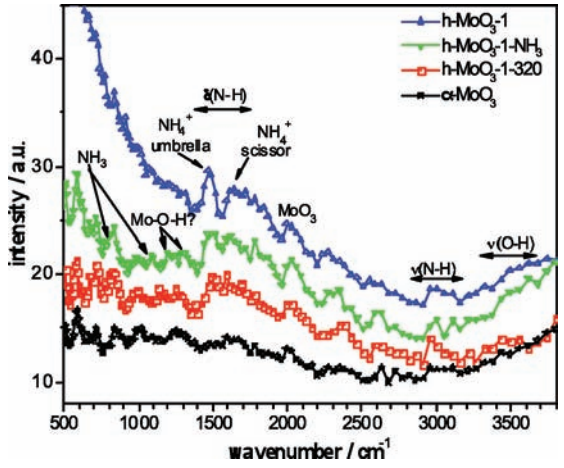

Figure 10. IINS spectra of hexagonal and orthorhombic MoO_3 (high wave number region).

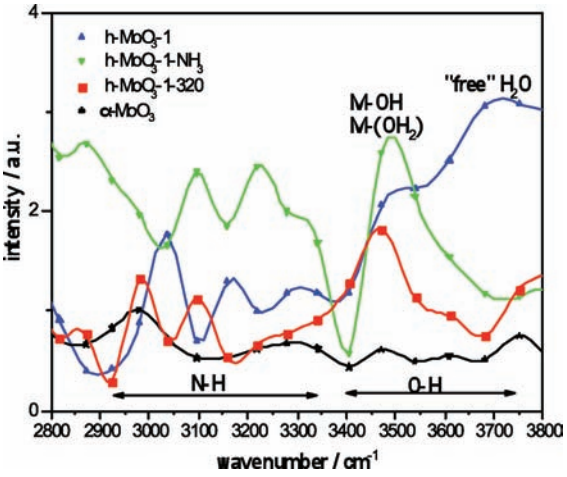

Figure 11. IINS spectra of hexagonal and orthorhombic MoO_3 (enlarged section of the range 2800−3800 cm^{-1}).

sample with most water (h-MoO_3-1) is a large area corresponding to "free" water clearly visible (arrow). After drying the sample over P_4O_{10} and loading it with dry gaseous ammonia, the free water seems to have been removed. The remaining water is either strongly adsorbed on the tunnel's surface or has reacted with the surface to form an aquo− or hydroxo−metal complex.

Figure 10 gives an overview of the fingerprint region. There is intensity visible in the expected areas for the $[NH_4]^+$ ion: N−H deformations (1380−1550 cm^{-1}, scissor at 1680 cm^{-1}; umbrella mode at 1400 cm^{-1}) and N−H stretch (3050−3350 cm^{-1}). For "free" ammonia NH_3, the N−H stretch and N−H scissor modes would be shifted to higher wave numbers (3223−3378 cm^{-1} and 1646 cm^{-1}, respectively). The umbrella mode, a very intense mode, should appear at 1060 cm^{-1}. We do, however, see an intense band at 1080 cm^{-1} for h-MoO_3-1-NH_3. Furthermore, a band at 800 cm^{-1} occurs as a shoulder in the same spectrum. This band could correspond to the rocking mode for NH_3, which occurs in the region 590−950 cm^{-1}. These observations agree with what we expected from the preparation route of this "ammoniated" sample.

Figure 11 is an enlarged section of the range 2800−3800 cm^{-1} where the N−H and O−H stretch frequencies appear. The data of the HEMO were treated slightly differently than before. The background that was subtracted from the sample spectra was the orthorhombic α-MoO_3 spectrum instead of the standard background vanadium. This can be done since at high wave numbers there are no phonon or lattice vibrations that differ in hexagonal and orthorhombic MoO_3 phases. By subtracting α-MoO_3, all Mo−O vibrational bands are eliminated, leaving the Mo−O−H and Mo−N−H vibrations more visible. The data points were connected using a cubic spline function to make the bands more distinguishable. The sample with the highest level of water, h-MoO_3-1, shows a large broad band from 3400 to 3800 cm^{-1}. This is common for lattice water (3200−3600 cm^{-1}: H−O−H stretch). The samples h-MoO_3-1-NH_3 and h-MoO_3-1-320 show a prominent band at 3480 cm^{-1} that indicates water strongly coordinated on a metal. The metal ion's charge and mass shift the frequencies to lower wave numbers. There are vibrational bands for N−H stretch in the region for $[NH_4]^+$ (3050−3350 cm^{-1}). The two N−H stretch vibrations of $[NH_4]^+$ shift to lower wave numbers from h-MoO_3-1-NH_3 (3220 and 3097 cm^{-1}) to h-MoO_3-1 (3170 and 3033 cm^{-1}) to h-MoO_3-1-320 (3101 and 2982 cm^{-1}).

The partially dehydrated samples h-MoO_3-1-320 and h-MoO_3-1-NH_3 are characterized by the near absence of clear librational bands for (nearly free) hydrogen-bonded water. On the other hand, the "free" water is only visible in h-MoO_3-1 (cf. Figure 9). Water in the other two hexagonal samples seems to have reacted and formed hydroxyl groups or was adsorbed onto the walls of the tunnels. When looking carefully, there is a sharp peak around 3500 cm^{-1} for h-MoO_3-1-NH_3 and h-MoO_3-1-320 (see Figure 11). The band around 3500 cm^{-1} is most likely the O−H stretch in Mo−OH or M−(OH_2) that is shifted to lower wave numbers due to the heavy metal Mo.

Due to the position and intensity of the bands, we conclude that there is ammonium $[NH_4]^+$ present. In addition to that, there are weak signals for ammonia in one of the three hexagonal samples, namely, h-MoO_3-1-NH_3. The band with the high intensity at 1478 cm^{-1}, present in all three samples, is the umbrella mode of $[NH_4]^+$. It may be slightly shifted due to recoil. It is too high in frequency to be the umbrella mode of ammonia, NH_3. There is intensity in the spectrum where the $[NH_4]^+$ scissors would be at 1642 cm^{-1}. This band has less intensity than the umbrella mode. The N−H stretch region again shows typical bands for the N−H stretch of ammonium ions, but we also observe N−H stretching bands for ammonia in sample MoO_3-1-NH_3. A shift of N−H stretch frequencies for ammonium in the three samples was observed. It seems that the $[NH_4]^+$ cations float more or less freely in h-MoO_3-1 but are more restricted in h-MoO_3-1-NH_3, which is filled with "free" NH_3 (shift of the N−H stretch to a higher frequency).

The situation in the HEMO seems similar to that of a zeolite. The $[NH_4]^+$ cations seem to float freely in the tunnels when the tunnel's surface is hydroxylated or hydrated. The proton of $[NH_4]^+$ hops now and then on Mo−OH, taking advantage of the electron density on the oxygen lone electron pair. If there were significant intermolecular interactions, the librational frequencies would be shifted downward appreciably.

The ^1H NMR spectrum of h-MoO_3-2 is shown in Figure 12a. Line-shape deconvolution indicates that there are three different proton-containing species in the original material. One environment is characterized by a relatively narrow peak at 5.8 ppm, another by a broader peak at 6.6 ppm. An extremely weak peak at 1.0 ppm (cf. Figure 12c) must be assigned to a third species. Only the peaks at 6.6 ppm and 1.0 ppm remain in the $[NH_4]^+$-free sample h-MoO_3-2-NOX (Figure 12b). We tentatively ascribe these environments to

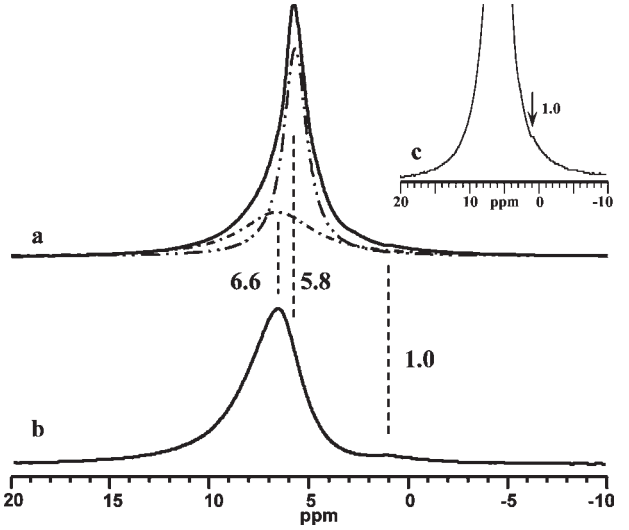

Figure 12. (a) ^{1}H MAS NMR spectrum of h-MoO_3-2 (the deconvolution of the spectral line profile is shown). (b) ^{1}H MAS NMR spectrum of h-MoO_3-2-NOX. (c) (Inset) Magnification of the weak peak at 1.0 ppm.

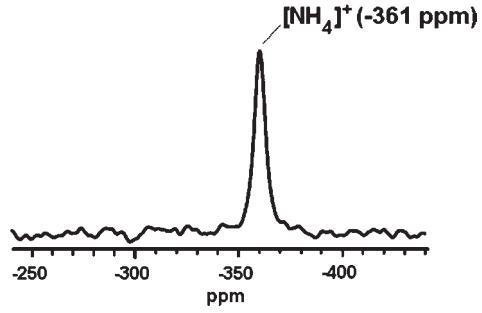

Figure 13. ^{15}N-CPMAS NMR spectrum of h-MoO_3-15N.

H_2O (resonates at 6.6 ppm), a $[NH_4]^+$-containing environment (resonates at 5.8 ppm), and isolated hydroxyl groups (resonate at 1.0 ppm).[36] We emphasize that proton exchange between all these environments is slow, relative to the NMR time scale of milliseconds, and the position of the peak attributed to water is not affected by the presence of $[NH_4]^+$. Thus, we assert that all three environments are not in contact with each other. We emphasize that protons of solitary water molecules resonate around 2 ppm, while water microdrops give rise to a peak at 4.8 ppm typical for liquid water.[37] Water molecules involved in stronger hydrogen bonds are characterized by higher values of the ^{1}H chemical shift. We attribute the observed chemical shift value of 6.6 ppm to an effect of the confined geometry of the HEMO.

The ^{15}N NMR spectrum of h-MoO_3-15N is shown in Figure 13. The chemical shift of −361 ppm confirms the findings of our other analytical methods. In addition to water molecules and OH groups, only $[NH_4]^+$ cations are located in the channels of the hexagonal structure. The reported chemical shifts for $^{15}NH_4Cl$ (aq) and $^{15}NH_4NO_3$ (aq) are −355.3 and −358.6,[38] and −358.5 ppm[39] for $^{15}NH_4NO_3$ (solid). The published data for $^{15}NH_3$ (liquid) and $^{15}NH_3$ (vapor) are −380.2 and −396.1 ppm.[40]

Conclusions

Considering all of the experimental data, the structure of the prepared parent polymeric "hexagonal molybdenum oxide" samples can best be described by the structural formula $(NH_4)_{x\infty}^{3}[Mo_y\square_{1-y}O_{3y}(OH)_x(H_2O)_{m-n}]\cdot nH_2O$ with $0.10 \leq x \leq 0.14$, $0.84 \leq y \leq 0.88$, and $m + n \geq 3 - x - 3y$. The hexagonal MoO_6 framework accommodate $[NH_4]^+$ cations, which float relatively freely in the structure's tunnels. In the neighborhood of vacant Mo sites, the terminal oxygen atoms are replaced either by H_2O molecules or OH^- groups.

The sample $MoO_3\cdot 0.326NH_3\cdot 0.343H_2O$, prepared by the ammoniation of a partially dehydrated $MoO_3\cdot 0.170NH_3\cdot 0.153H_2O$ with dry gaseous ammonia, accommodates NH_3 in the hexagonal tunnels, in addition to $[NH_4]^+$ cations and H_2O.

The "chimie douce" reaction with NO/NO_2 is able to remove topotactically all of the $[NH_4]^+$ cations at 100 °C from the parent structure. This result demonstrates that the *in situ* oxidation of $[NH_4]^+$ is an elegant route for preparing metastable oxides with tunnels for various applications in the field of batteries and catalysis.

The structural type of "hexagonal molybdenum oxide" is characterized by an extended phase range, which led many authors to erroneous interpretations of their experimental findings.

Acknowledgment. We are indebted to Prof. Dr. Dieter Lentz from Freie Universität Berlin for helpful discussions.

Supporting Information Available: Crystallographic data for hexagonal molybdenum oxide in CIF format. This material is available free of charge via the Internet at http://pubs.acs.org.

(36) Mauder, D.; Akcakayiran, D.; Lesnichin, S. B.; Findenegg, G. H.; Shenderovich, I. G. *J. Phys. Chem. C* **2009**, *113*, 19185–19192.

(37) Nakahara, M.; Wakai, C. *Chem. Lett.* **1992**, *5*, 809–812.

(38) Srinivasan, P. R.; Lichter, R. L. *J. Magn. Reson.* **1977**, *28*, 227–234.

(39) Hayashi, S.; Hayamizu, K. *Bull. Chem. Soc. Jpn.* **1991**, *64*, 688–690.

(40) Litchman, W. M.; Alei, M., Jr.; Florin, A. E. *J. Am. Chem. Soc.* **1969**, *91*, 6574–6579.